

A substructure isolation method for local structural health monitoring*

Jilin Hou^{1,2}, Łukasz Jankowski^{2,*} and Jinping Ou^{1,3,*}

¹ School of Civil Engineering, Harbin Institute of Technology, Harbin 150090, P. R. of China

² Smart-Tech Centre, Institute of Fundamental Technological Research, Polish Academy of Sciences, Warsaw, Poland

³ School of Civil and Hydraulic Engineering, Dalian University of Technology, Dalian 116024, P. R. of China

SUMMARY

This paper describes an effective method of substructure isolation for local structural health monitoring (SHM). In practice, often only a small part of a larger structure is critical and needs monitoring. However, typical low-frequency SHM methods require modeling and analysis of the global structure, which can be costly, time-consuming and error-prone. The proposed approach is based on the virtual distortion method (VDM) and uses force distortions to model fixed supports in the boundary nodes to isolate the considered substructure from influences of the rest of the structure. Therefore, given an excitation of the substructure and the measured response of the global structure, the response of the substructure treated as fixed supported can be computed. Local-only monitoring is then possible using virtually any of the existing methods. However, consistently with the isolation methodology, strain distortions are used here for modeling of damages of the isolated substructure. The discrete adjoint variable method is used for the first time within the framework of the VDM in order to perform quick analytical sensitivity analysis and improve the computational effectiveness of the damage identification by one order of magnitude. A numerical experiment of a frame-truss is presented to validate the methodology at 5% rms measurement error level. Copyright © 2002 John Wiley & Sons, Ltd.

KEY WORDS: Substructure isolation; Damage identification; Virtual Distortion Method; Structural health monitoring; Adjoint variable method

1. INTRODUCTION

In recent years, Structural Health Monitoring (SHM) has become a widely researched field in civil engineering, see e.g. [1, 2]. The primary task of an SHM system is damage detection and identification. However, as science and technology develop, structures become larger and more complex, and it is increasingly harder to pursue damage identification using standard global methods, which require considering the monitored structure in its entirety. On the other hand, in many practical applications

*This is the **pre-peer reviewed version** of the following article: J. Hou, Ł. Jankowski, J. Ou, A substructure isolation method for local structural health monitoring, *Journal of Structural Control & Health Monitoring*, in press, 10.1002/stc.389, which has been published in final form at <http://dx.doi.org/10.1002/stc.389>

*Correspondence to: oujinpjng@hit.edu.cn (substructure isolation), lukasz.jankowski@ippt.gov.pl (virtual distortion method)

only small substructures are considered crucial, so that local monitoring for damages would be sufficient as well as less expensive. Therefore, there is a need for methods, which would allow local-only information to be extracted from measured response of the global structure, so that it can be used for substructure monitoring and local damage identification.

The substructure isolation method proposed in this paper uses virtual force distortions in order to numerically counter the influences of the rest of the structure on the monitored substructure (another formulations are proposed in [3, 4, 5]). The force distortions are applied in such a way that all degrees of freedom (DOFs) of the substructure boundary behave as fixed supported. In this way the considered substructure is fully isolated from the global structure and, in response to local excitations, can be treated as a new independent, simpler and smaller structure, so that its monitoring and analysis become much easier.

The concept of using virtual (force and strain) distortions for modeling of structural modifications is the core idea of the virtual distortion method (VDM) [6, 7, 8]. To date, force distortions have been used to model mass-related modifications and environmental damping, while strain distortions have been applied to model stiffness-related defects or modifications, structural damping [9], delamination [10] and to identify unknown coexistent loads and damages [11]. In this paper, it is proposed to use force distortions to model another kind of structural modification: *fixed support*. A series of such modeled fixed supports, if placed in all boundary modes of the considered substructure, amounts to the elimination of all influences of the rest of the structure and thus to complete *substructure isolation*. In this way, local-only analysis and monitoring of the isolated substructure as well as damage identification are made feasible.

Practical implementation of the substructure isolation approach considered here is relatively simple due to its two important features:

1. Force distortions need not be impulsive, so that raw measurements, e.g. of an impulse hammer can be directly used. This is in contrast to many earlier inverse methods, which (with the exception of the model-free approach of [12]) require either a well-tuned numerical model of the global structure [7] or troublesome ill-posed deconvolution of the measurement data [13].
2. When used for substructure isolation, force distortions need not to be applied exactly in its boundary DOFs. In fact, all DOFs of the exterior global structure can be used for this purpose as long as the respective influence matrix (which relates the boundary responses to the distortions) is not rank-deficient. This is an extension to other distortion-based approaches, which require the distortions to be applied exactly in all DOFs of the affected elements or nodes.

The virtual distortion method (VDM) itself belongs to the class of fast reanalysis methods [14]. Given the response of the original unmodified structure to a given excitation, the VDM allows the effect of localized structural modifications to be quickly computed without a repeated global simulation of the entire structure. Instead, the influence of the modifications on the structural response is expressed in the form of a convolution of virtual distortions with impulse-responses to excitations at the locations of the considered modifications. These impulse-responses encode all the necessary information about the influence of the modifications on the structural response, and are stored in the hence so-called *dynamic influence matrices*. The virtual distortions are imposed on the unmodified structure in order to model the modifications, and have to be computed by solving a convolution-type equation, which is usually computationally much less expensive than updating the entire structural model and performing a global simulation of the modified structure. An important advantage of the VDM is its ability of analytical sensitivity analysis, which allows quick gradient-based optimization techniques to be used in SHM-related inverse damage identification problems. However, up to now only the direct

differentiation method of sensitivity analysis has been used [6, 7]. This paper introduces the adjoint variable method [15] to the VDM, which allows the computational costs of identification to be reduced by one order of magnitude.

The paper is structured as follows. The next section describes the use of force distortions for modeling of arbitrarily placed fixed supports, while their application to substructure isolation is discussed in the third section. The fourth section concisely refers the VDM-based approach to identification of stiffness-related damages and introduces the adjoint variable method into this context. The numerical example of the last section tests the methodology on a modeled frame-truss structure; the feasibility of the approach is demonstrated at the assumed Gaussian measurement error level of 5% rms.

2. MODELING OF FIXED SUPPORTS

In agreement with the general approach of the VDM, the structural response of a *modified structure* (i.e. the original structure with a number of fixed supports added) to an external load is expressed in the form of a combination of the responses of the original structure to (1) the same load (*measured response*) and to (2) certain virtual force distortions that act in all DOFs of the nodes with modeled supports to model the support forces (called the *residual response*). The original structure with supports modeled by distortions will be called the *distorted structure*. The assumptions of linearity and small deformations are required in order to allow the responses to be linearly combined.

The force distortions can be computed using the condition that the modeled responses in the all nodes with modeled fixed supports vanish. Thereupon, the responses of the considered sensors can be computed by using the same principle of superposition of the measured response of the original structure and the responses to the (already known) distortions.

2.1. Response of the distorted structure

Assume that the distorted structure is externally loaded, denote by $a_i(t)$ its discretized response (displacement, velocity or acceleration) in the i th DOF and by $\varepsilon_\alpha(t)$ the discretized response of the α th sensor. With the zero initial conditions and discretized time, both responses can be expressed as the following sums of the measured and the residual parts

$$a_i(t) = a_i^M(t) + \sum_j \sum_{\tau=0}^t B_{ij}^0(t-\tau) f_j^0(\tau), \quad (1)$$

$$\varepsilon_\alpha(t) = \varepsilon_\alpha^M(t) + \sum_j \sum_{\tau=0}^t D_{\alpha j}^0(t-\tau) f_j^0(\tau), \quad (2)$$

where i and j index only the DOFs of the nodes with modeled fixed supports, α indexes the sensors, $f_j^0(t)$ denotes the virtual force distortion in the j th DOF, while $B_{ij}^0(t)$ and $D_{\alpha j}^0(t)$ denote the system impulse-responses (influence matrices), which relate the virtual force in the j th DOF to the responses in the i th DOF and of the α th sensor, respectively. The measured responses of the original structure are denoted by $a_i^M(t)$ and $\varepsilon_\alpha^M(t)$. Equations 1 and 2, rewritten for the all considered values of the indices,

take in the matrix notation the following form of two large linear systems

$$\mathbf{a} = \mathbf{a}^M + \mathbf{B}^0 \mathbf{f}^0, \quad (3)$$

$$\boldsymbol{\varepsilon} = \boldsymbol{\varepsilon}^M + \mathbf{D}^0 \mathbf{f}^0, \quad (4)$$

where, with proper ordering of the unknown distortions, \mathbf{B}^0 and \mathbf{D}^0 take the form of large block matrices with Toeplitz blocks.

If the force distortions \mathbf{f}^0 are assigned such values that they properly model the effects of the fixed supports in the chosen nodes, then (4) can be directly used to compute the sensor measurements of the modified structure. Since the responses in all DOFs of the fixed supported nodes vanish, that is $\mathbf{a} = \mathbf{0}$ in (3), the proper numerical values of the force distortions can be found by solving the following square linear system:

$$\mathbf{B}^0 \mathbf{f}^0 = -\mathbf{a}^M. \quad (5)$$

The solution to (5) can be computed using any of the direct or iterative methods, the latter may be more effective in the cases of many time steps and a large matrix \mathbf{B}^0 . In this paper, the solution is computed directly using the pseudoinverse matrix as

$$\mathbf{f}^0 = -[\mathbf{B}^0]^+ \mathbf{a}^M, \quad (6)$$

which, upon substitution into (4), yields the following formula for the modeled sensor measurements:

$$\boldsymbol{\varepsilon} = \boldsymbol{\varepsilon}^M - \mathbf{D}^0 [\mathbf{B}^0]^+ \mathbf{a}^M. \quad (7)$$

In practice the matrix \mathbf{B}^0 is usually ill-conditioned, hence its pseudoinverse has to be regularized. In this paper, the truncated singular value decomposition (TSVD) is used.

2.2. Application-oriented formulation

Given an external excitation, the responses $\boldsymbol{\varepsilon}^M$ and \mathbf{a}^M are *measured experimentally* by the considered sensors (indexed by α) and by additional dedicated sensors placed in the degrees of freedom of the nodes with modeled fixed supports, respectively. Equation 7 can be then used to compute the response of the modified structure, provided the corresponding system impulse-responses $D_{ij}^0(t)$ and $B_{ij}^0(t)$ are both known.

However, in the intended practical applications to isolation of local substructures in large and complex real-world structures, the model of the entire structure cannot be assumed to be available and so the exact impulse-responses cannot be assumed to be known. Nevertheless, it can be possible to measure experimentally the responses $B_{ij}(t)$ and $D_{\alpha j}(t)$ of the structure to given non-impulsive excitations $f_j(t)$ in all j -indexed DOFs of the nodes considered for fixed supports. Although the impulse-responses $B_{ij}^0(t)$ and $D_{\alpha j}^0(t)$ could be then obtained by a deconvolution, it would amount to solving a number of linear equations of the first kind with compact integral operators, which is a necessarily ill-posed problem [16]. Therefore, it is proposed here to use directly the experimentally measured responses $B_{ij}(t)$, $D_{\alpha j}(t)$ and $f_j(t)$, by expressing the virtual force $f_j^0(t)$ as the following combination of the experimentally used non-impulsive excitation $f_j(t)$ with a series of combination coefficients $c_j(t)$,

$$f_j^0(t) = \sum_{\tau=0}^{T-1} f_j(t-\tau) c_j(\tau), \quad (8)$$

where T is the considered number of the time steps. The formulas (1) and (2) for the system responses, instead of the unknown impulse-responses, can be then formulated using the *experimentally measured* responses as

$$a_i(t) = a_i^M(t) + \sum_j \sum_{\tau=0}^{T-1} B_{ij}(t-\tau)c_j(\tau), \quad (9)$$

$$\varepsilon_\alpha(t) = \varepsilon_\alpha^M(t) + \sum_j \sum_{\tau=0}^{T-1} D_{\alpha j}(t-\tau)c_j(\tau). \quad (10)$$

Since the experimental excitations $f_j(t)$ are non-impulsive, the upper summation limits in (9) and (10) had to be extended from t to $T-1$ and can be set back to t only if $f_j(t) = 0$ for all j and all $t < 0$. As before, both equations can be stated in the matrix form,

$$\mathbf{a} = \mathbf{a}^M + \mathbf{B}\mathbf{c}, \quad (11)$$

$$\boldsymbol{\varepsilon} = \boldsymbol{\varepsilon}^M + \mathbf{D}\mathbf{c}, \quad (12)$$

and used to compute the responses of the considered sensors using purely experimental data as

$$\boldsymbol{\varepsilon} = \boldsymbol{\varepsilon}^M - \mathbf{D}\mathbf{B}^+\mathbf{a}^M, \quad (13)$$

where \mathbf{B}^+ is the (regularized) pseudoinverse of the matrix \mathbf{B} . The Toeplitz block structure of the matrices \mathbf{B} and \mathbf{D} is illustrated in Figure 4.

3. SUBSTRUCTURE ISOLATION

A series of properly placed modeled fixed support can be used to isolate numerically a substructure from the rest of the global structure by eliminating all external influences. Given a substructure, the modeled fixed supports have to be placed in all nodes of its boundary, so that all responses of the related degrees of freedom vanish. The isolated substructure behaves then as fixed supported and responses by (13) to local excitations only.

In the discussed above case of arbitrarily placed fixed supports, the virtual force distortions had to be applied in all degrees of freedom of all nodes with modeled fixed supports. However, when the approach is applied to substructure isolation and local monitoring, only the local response of the considered substructure matters and all sensors are placed either on its boundary (to measure $a_i^M(t)$) or in its interior (to measure $\varepsilon_\alpha^M(t)$). Therefore, since the response of the rest of the global structure is of no interest, the virtual force distortions can be applied in principle *anywhere outside the substructure*, that is external degrees of freedom of the global structure can be also used for this purpose, besides the degrees of freedom of the substructure boundary. It should be only required that the placement of the distortions allows the substructure boundary to be constrained, which can be expressed in the form of the requirement that the influence matrix \mathbf{B} (constructed of the experimentally measured i -indexed responses of the boundary degrees of freedom to the experimentally used non-impulsive excitations $f_j(t)$) is not rank-deficient. It is a considerable simplification with practical consequences, since in real-world structures not all degrees of freedom of the boundary of the considered substructure can be expected to be accessible for experimental excitation.

4. LOCAL DAMAGE MONITORING

Virtual distortions are the core idea of the VDM [6, 7, 8], which uses them for modeling and identification of structural damages. For reasons of notational simplicity, the concept is referred here only for elastic trusses and stiffness-related damages, although it is applicable in a similar way to other types of structures and damage patterns [6, 17], provided the damage preserves the linearity of the structure, which is required for the isolation process. The quick sensitivity analysis with the adjoint variable method is introduced in the last subsection.

4.1. Virtual strain distortions

Using the approach of the VDM, the damaged isolated substructure is modeled by the distorted isolated substructure (the intact isolated system subjected to the same excitation and certain virtual distortions), which is equivalent in terms of identical strains and internal forces. Stiffness-related damages are modeled by virtual strain distortions, that is by additionally introduced strains. In the case of a truss element, the virtual strain distortion is modeled by a pair of self-equilibrated forces applied axially at its nodes so that in the static case the element is respectively elastically strained. In the dynamic case the distortions and the corresponding forces are time-dependent.

If the small deformation case is assumed, the strain response $\varepsilon_\alpha(t)$ of the α th sensor to a force excitation of the distorted isolated substructure can be expressed in the form similar to (10) as

$$\varepsilon_\alpha^D(t) = \varepsilon_\alpha^L(t) + \sum_{\beta} \sum_{\tau=0}^t H_{\alpha\beta}^0(t - \tau) \varepsilon_\beta^0(\tau), \quad (14)$$

where $\varepsilon_\alpha^L(t)$ denotes the response of the same sensor to the same excitation in the intact isolated substructure (called the *linear response*) and $\varepsilon_\beta^0(t)$ denotes the virtual distortion that is imposed on the β th element in order to model its stiffness-related damage. The influence matrix, that is the discretized impulse-response of the intact isolated substructure, is denoted by $H_{\alpha\beta}^0(t)$ and, if necessary, can be replaced using experimentally measured responses by a convolution similar to (8) and (13).

4.2. Stiffness modification coefficients

Let μ_α denote the stiffness modification coefficient of the α th element of the substructure, that is the ratio of its modified Young's modulus to the original modulus:

$$\mu_\alpha = \frac{\hat{E}_\alpha}{E_\alpha}. \quad (15)$$

The virtual strain distortions $\varepsilon_\beta^0(t)$ in (14) can be related to the stiffness modification coefficients by the requirement of equality of the element forces in the damaged and distorted isolated substructures, which can be stated as

$$\hat{E}_\beta A_\alpha \varepsilon_\alpha^D(t) = E_\alpha A_\alpha [\varepsilon_\alpha^D(t) - \varepsilon_\alpha^0(t)], \quad (16)$$

where A_α denotes the cross-sectional area of the α th element and is assumed to be invariant (otherwise the mass of the element is affected, which has to be modeled with a separate force distortion). Equations 15 and 16 yield together

$$\varepsilon_\alpha^0(t) = [1 - \mu_\alpha(t)] \varepsilon_\alpha^D(t). \quad (17)$$

Equation 14, substituted into (17), yields the following linear system:

$$\sum_{\beta} [\delta_{\alpha\beta} - (1 - \mu_{\alpha})H_{\alpha\beta}^0(0)] \varepsilon_{\beta}^0(t) = (1 - \mu_{\alpha})\varepsilon_{\alpha}^L(t) + (1 - \mu_{\alpha}) \sum_{\tau=0}^{t-1} \sum_{\beta} B_{\alpha\beta}(t - \tau) \varepsilon_{\beta}^0(\tau), \quad (18)$$

where $\delta_{\alpha\beta}$ denotes Kronecker's delta and the unknowns are the force distortions $\varepsilon_{\beta}^0(t)$. Equation 18 can be solved iteratively with respect to time steps $t = 0, 1, \dots, T - 1$; upon the solution, the response $\varepsilon_{\alpha}^D(t)$ of the distorted isolated substructure can be computed directly by (14).

4.3. Damage identification and sensitivity analysis

Given the measured response $\varepsilon_{\alpha}^M(t)$ and $a_i^M(t)$ of the damaged global structure to an external load, the response $\varepsilon_{\alpha}(t)$ of the damaged isolated substructure can be computed by (13) and compared to the response $\varepsilon_{\alpha}^D(t)$ modeled by (14) in order to construct the following objective function:

$$F(\mu_1, \mu_2, \dots) = \frac{1}{2} \sum_{\alpha} \sum_{t=0}^{T-1} d_{\alpha}^2(t), \quad d_{\alpha}(t) = \varepsilon_{\alpha}(t) - \varepsilon_{\alpha}^D(t), \quad (19)$$

which depends on the stiffness modification coefficients μ_{α} via the modeled response $\varepsilon_{\alpha}^D(t)$. The objective function F measures the discrepancy between the measured response of the damaged isolated substructure (more precisely, the response computed based on the measurements of the damaged global structure) and the response modeled for given modification coefficients μ_{γ} .

Identification of the damage amounts to minimization of the objective function F , and can be performed quickly using gradient-based optimization algorithms, provided the gradient can be computed at a reasonable cost. By the direct substitution of the differentiated (14) into the differentiated objective function (19), the derivative of the objective function is expressed in terms of the derivatives of the virtual distortions,

$$\frac{\partial F}{\partial \mu_{\gamma}} = - \sum_{t=0}^{T-1} \sum_{\alpha} d_{\alpha}(t) \sum_{\tau=0}^t \sum_{\beta} H_{\alpha\beta}^0(t - \tau) \frac{\partial \varepsilon_{\beta}^0(\tau)}{\partial \mu_{\gamma}}. \quad (20)$$

Up to now [6, 7], the gradient of the objective function has been computed by the direct differentiation method, that is by iterative solution of the differentiated (18),

$$\sum_{\beta} [\delta_{\alpha\beta} - (1 - \mu_{\alpha})H_{\alpha\beta}^0(0)] \frac{\partial \varepsilon_{\beta}^0(t)}{\partial \mu_{\gamma}} = -\delta_{\alpha\gamma}\varepsilon_{\alpha}(t) + (1 - \mu_{\alpha}) \sum_{\tau=0}^{t-1} \sum_{\beta} H_{\alpha\beta}^0(t - \tau) \frac{\partial \varepsilon_{\beta}^0(\tau)}{\partial \mu_{\gamma}}, \quad (21)$$

and by substitution of the obtained derivatives of the virtual distortions into (20). Equation 21 has to be solved separately for every considered stiffness modification coefficient. Therefore, with the direct method, the time complexity of the sensitivity analysis is linear with respect to the number of the potentially damaged elements.

This paper introduces the adjoint variable method [15] into the VDM, which requires only a single solution of the adjoint equation (equal in size to (21)) and thus makes the numerical costs of the sensitivity analysis small and practically constant, irrespective of the number of the stiffness modification coefficients. In order to eliminate from (20) the explicit dependence on the derivatives of the distortions, (21) is first multiplied by the adjoint variable $\lambda_{\alpha}(t)$ and summed with respect to t

and α . After interchanging the order of summation, it yields

$$0 = \sum_{t=0}^T \lambda_{\gamma}(t) \varepsilon_{\gamma}(t) + \sum_{t=0}^{T-1} \sum_{\alpha} \left[\lambda_{\alpha}(t) - \sum_{\beta} (1 - \mu_{\beta}) \sum_{\tau=t}^{T-1} \lambda_{\beta}(\tau) B_{\beta\alpha}(\tau - t) \right] \frac{\partial \varepsilon_{\alpha}^0(t)}{\partial \mu_{\gamma}}. \quad (22)$$

By interchanging the order of summation in (20) and adding the result to (22), the following formula is obtained:

$$\begin{aligned} \frac{\partial F}{\partial \mu_{\gamma}} = \sum_{t=0}^{T-1} \lambda_{\gamma}(t) \varepsilon_{\gamma}(t) + \sum_{t=0}^{T-1} \sum_{\alpha} \left[\lambda_{\alpha}(t) - \sum_{\beta} (1 - \mu_{\beta}) \sum_{\tau=t}^{T-1} \lambda_{\beta}(\tau) H_{\beta\alpha}^0(\tau - t) \right. \\ \left. - \sum_{\tau=t}^{T-1} \sum_{\beta} d_{\beta}(\tau) H_{\beta\alpha}^0(\tau - t) \right] \frac{\partial \varepsilon_{\alpha}^0(t)}{\partial \mu_{\gamma}}. \end{aligned} \quad (23)$$

The adjoint variable $\lambda_{\alpha}(t)$ can be assigned such values that the terms in the square brackets vanish. As the result,

$$\frac{\partial F}{\partial \mu_{\gamma}} = \sum_{t=0}^{T-1} \lambda_{\gamma}(t) \varepsilon_{\gamma}(t), \quad (24)$$

where the adjoint variable satisfies

$$\begin{aligned} \sum_{\beta} [\delta_{\alpha\beta} - (1 - \mu_{\beta}) H_{\beta\alpha}^0(0)] \lambda_{\beta}(t) = \sum_{\tau=t}^{T-1} \sum_{\beta} d_{\beta}(\tau) H_{\beta\alpha}^0(\tau - t) \\ + \sum_{\beta} (1 - \mu_{\beta}) \sum_{\tau=t+1}^{T-1} \lambda_{\beta}(\tau) H_{\beta\alpha}^0(\tau - t). \end{aligned} \quad (25)$$

Equation 25 can be solved iteratively, backward with respect to time, for $t = T - 1, \dots, 1, 0$. Note that for the sensitivity analysis only a single solution of (25) is necessary, irrespective of the number of potential damages.

5. NUMERICAL EXAMPLE

A plain frame-truss structure shown in Figure 1(a) was taken as an example to test the application of the proposed methodology of substructure isolation and local damage monitoring. The structure consists of two parts: the top is a stiff frame which neglects axial distortions, the bottom consists of its two supports which are 11-element trusses. The right truss is the considered substructure.

The entire structure is 6 m wide and 6 m high, originally made of steel with density 7800 kg/m³ and Young's modulus 210 GPa. The cross-sections of the truss bars and the frame beams are 63 cm² and 120 cm², respectively. The inertia moments of all frame beams is 9330 cm⁴. The Rayleigh damping model is assumed with both damping ratios equal to 1%.

The global structure consists of 31 elements, its damage was simulated by reducing their stiffnesses. The assumed damage extents (that is the stiffness reduction ratios μ_{α} , see (15)) are shown in Figure 2, the first 11 of them relate to the considered substructure. It has been assumed that all damage extents are unknown, but only the first 11 are to be identified.

Sensor placement is shown in Figure 1(b). Three acceleration sensors (denoted by b_1 , b_2 and b_3) were placed in the three degrees of freedom of the substructure boundary, so that they can be used for the isolation. The strain sensors 1, 2 and 3 were placed in the interior of the substructure, so that they can be used for its local monitoring and identification of the damage.

5.1. Response of the isolated substructure

The model of the isolated undamaged substructure was assumed to be available, so that it could serve as the reference for damage identification (in practice, the model would have to be identified before the damage occurs, using the same isolation method). Natural frequencies of the intact substructure are listed in Table I. The sampling frequency was chosen to be 10000 Hz in order to guarantee that the sampled data contain all the necessary dynamic information about the substructure. The total considered time was $T = 10$ ms, and has been discretized into 100 time steps of $\Delta t = 0.1$ ms.

In order to compute by (13) the sensor responses of the isolated damaged substructure, which is shown in Figure 1(c), two previous steps were necessary.

First, the entire structure was excited successively at the locations of the boundary sensors (that is in all boundary degrees of freedom). Their responses and the responses of the interior strain sensors were then used to construct the matrices \mathbf{B} and \mathbf{D} , respectively. The excitations used to this end are denoted by f_{e1} , f_{e2} and f_{e3} , they simulate modal hammer excitations and are shown in Figure 3(abc) together with the corresponding responses of the boundary and interior sensors. The matrices \mathbf{B} and \mathbf{D} have the block Toeplitz structure, which is illustrated in Figure 4. Note that only the responses are required for the isolation process; the excitations are plotted here for illustrative purposes only, but are not used in the computations.

Second, given the matrices \mathbf{B} and \mathbf{D} , the response of the isolated damaged substructure to any test excitation can be computed by (13) using the response vectors $\boldsymbol{\varepsilon}^M$ and \mathbf{a}^M of the entire damaged structure. The test excitation used in this numerical example simulates a longitudinal piezo-excitation and acts at the location of sensor 1. The excitation is plotted in Figure 3(d), besides the recorded responses of the boundary sensors (b_1 , b_2 and b_3) and of the interior sensors (1, 2 and 3), which are used to construct the response vectors \mathbf{a}^M and $\boldsymbol{\varepsilon}^M$, respectively. Note that, in this step, both the computed response $\boldsymbol{\varepsilon}$ and the test excitation are necessary for the purposes of substructure monitoring and damage identification.

Figure 5 shows the computed response $\boldsymbol{\varepsilon}$ of the isolated damaged substructure (dotted lines) and compares it to the response obtained directly from its theoretical model (solid lines), which is assumed to be unknown for monitoring purposes. The responses are virtually undistinguishable, which testifies the successful isolation of the concerned substructure. The damage extents are identified by comparing these responses to the reference response of the undamaged isolated substructure, which is also plotted in Figure 5 (dashed line).

5.2. Damage identification

The damage extents of the elements of the substructure have been identified by minimizing the objective function (19). In this section, no measurement error is taken into account and the computed responses are assumed to be accurate. Figure 6 compares the identified and the actual (assumed) damage extents.

Note that, because the concerned substructure was numerically isolated from the global structure, there were only 11 unknown parameters that needed to be identified instead of 31 parameters related to all elements of the entire structure. In cases of large and complex real-world structures this reduction

will be much larger and more significant. The isolation process decreases therefore the numerical cost of the optimization and, in this way, increases the chances to obtain high accuracy of the damage identification.

5.3. Influence of measurement error

In practice, the measurement error is unavoidable. Its effect on the identification accuracy is tested in this section by polluting the simulated responses with numerically generated uncorrelated Gaussian noise at the 5% rms level.

In order to test the influence of the measurement error on the accuracy of the identified damages, five different cases have been considered, see Table II. The cases include the noise pollution of all involved structural responses (\mathbf{a}^L , ϵ^L and ϵ^M), of the force excitation used for damage identification, and an additional initial data denoising using built-in Matlab function “wden” with standard settings. In Table II, the symbols s and f collectively denote the sensor responses and the force excitation, respectively. The subscripts mark the level of the simulated error, while the superscript “w” is used to denote that the signal has been denoised before processing. As an example, Figure 7 plots the noise-polluted and denoised excitation and responses corresponding to the noise-free plots of Figure 3(d).

The responses of the isolated damaged substructure are computed based on the noise-polluted and denoised measurements (cases $s_{5\%}$ and $s_{5\%}^w$) and compared in Figure 8 with the responses obtained using the noise-free measurements. The damage extents corresponding to all five considered cases have been identified, the results are shown in Figure 9. Despite the simulated measurement error at 5% rms level, the damage extents are in all tested cases identified relatively accurately. Moreover, the initial denoising of the measurements have improved the identification accuracy.

6. CONCLUSIONS

This paper presents an efficient and implementation-ready method for local structural health monitoring that can be applied for damage identification of chosen simple, small substructures of large and complex global structures.

The considered substructure is isolated from the entire structure by placing modeled fixed supports in all nodes of their mutual boundary. The influence of the rest of the structure is filtered out using experimental data only, no numerical modeling is required for the isolation process. In this way local-only, substructure-pertinent information can be extracted from the measured response of the entire structure. The computed response of the isolated substructure can be then used for its local-only analysis and damage identification using a variety of existing methods. The computational cost of such a local analysis is significantly reduced in comparison to the cost of the analysis of the entire structure.

Consistently with the isolation methodology, strain distortions and the Virtual Distortion Method (VDM) are applied for modeling of damages of the isolated substructure. Quick analytical sensitivity analysis and damage identification are made possible by introducing for the first time the discrete adjoint method into the VDM.

The isolation method in the proposed form is limited to linear damages. This does not appear to be a significant restriction of its applicability, since most of the practical damages in civil engineering seem to be linear. However, a generalization to nonlinear cases is going to be investigated in further research.

ACKNOWLEDGEMENTS

The authors gratefully acknowledge the support of the Key Project of Natural Science Foundation of China #50538020, of the Project of National Key Technology R&D Program (China) #2006BAJ03B05 and of Polish Research Project PILOT no. *to be provided later*.

REFERENCES

1. Ou J. Research and practice of smart sensor networks and health monitoring systems for civil infrastructures in mainland China. *Bulletin of National Natural Science Foundation of China* 2005; **19**(1):8–12.
2. Kołakowski P. Structural Health Monitoring — a Review with the Emphasis on Low-Frequency Methods. *Engineering Transactions* 2007; **55**(3):1–37.
3. Hou J, Ou J. Isolated Substructure Model Updating Method Based on Local Impulse Response. submitted to *Engineering Mechanics* (in Chinese) 2009.
4. Hou J, Ou J. Isolated Substructure Model Updating Method Based on Local Mode. submitted to *Chinese Journal of Theoretical and Applied Mechanics* (in Chinese) 2009.
5. Hou J, Ou J. Isolated Substructure Model Updating Method Based on Local Time Series. *Journal of Vibration Engineering* (in Chinese) 2009; in press.
6. Holnicki-Szulc J. (ed.) *Smart Technologies for Safety Engineering*. John Wiley & Sons Ltd, Chichester, 2008.
7. Kołakowski P, Wikło M, Holnicki-Szulc J. The virtual distortion method — a versatile reanalysis tool for structures and systems. *Structural and Multidisciplinary Optimization* 2008; **36**(3):217–234.
8. Holnicki-Szulc J, Gierliński J. *Structural Analysis, Design and Control by the Virtual Distortion Method*. John Wiley & Sons Ltd, Chichester, 1995.
9. Mróz M, Holnicki-Szulc J. Remodelling of vibrating systems via frequency-domain-based virtual distortion method. *Mechanics* 2005; **24**(2):124–129.
10. Orłowska A, Kołakowski P, Holnicki-Szulc J. Modelling and identification of delamination in double-layer beams by the virtual distortion method. *Computers & Structures* 2008; **86**(23–24):2203–2214.
11. Zhang Q, Jankowski Ł, Duan Z. Identification of coexistent load and damage. *Structural and Multidisciplinary Optimization* 2009; in review.
12. Suwała G, Jankowski Ł. A model-less method for added mass identification. *Solid State Phenomena* 2009; **147–149**:570–575.
13. Inoue H, Harrigan JJ, Reid SR. Review of inverse analysis for indirect measurement of impact force. *Applied Mechanics Reviews* 2001; **54**(6):503–524.
14. Akgün MA, Garcelon JH, Haftka RT. Fast exact linear and non-linear structural reanalysis and the Sherman-Morrison-Woodbury formulas. *International Journal for Numerical Methods in Engineering* 2001; **50**(7):1587–1606.
15. Kleiber M, Antunez H, Kowalczyk P. *Parameter Sensitivity in Nonlinear Mechanics: Theory and Finite Element Computations*. John Wiley & Sons Ltd, Chichester, 1997.
16. Kress R. *Linear integral equations*. Springer, New York, 1989.
17. Putresza JT, Kołakowski P. Sensitivity analysis of frame structures — Virtual Distortion Method approach. *International Journal for Numerical Methods in Engineering* 2001; **50**(6):1307–1329.

Table I. The first 8 natural frequencies of the intact isolated substructure

No.	1st	2nd	3rd	4th	5th	6th	7th	8th
Eigenfrequency [Hz]	214.2	457.2	638.9	804.4	1090.4	1160.5	1336.9	1397.0

Table II. Five considered cases of noise pollution

case 1	case 2	case 3	case 4	case 5
$s_{0\%}$ and $f_{0\%}$	$s_{5\%}$ and $f_{0\%}$	$s_{5\%}^w$ and $f_{0\%}$	$s_{5\%}$ and $f_{5\%}$	$s_{5\%}^w$ and $f_{5\%}^w$

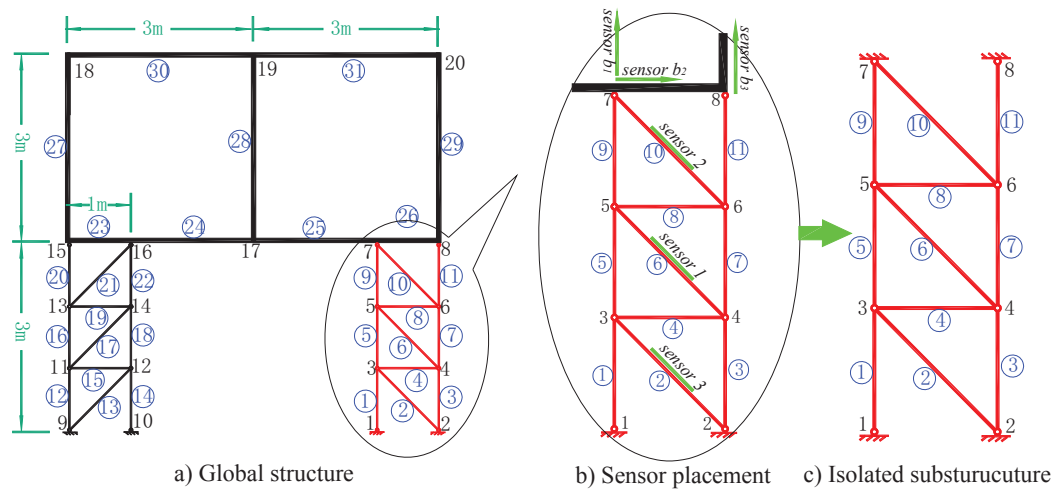


Figure 1. Global structure, sensor placement and isolated substructure

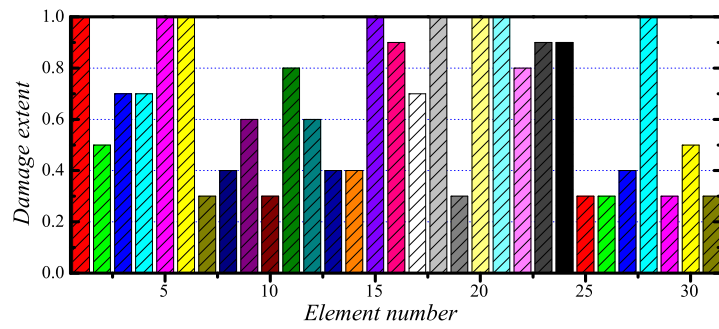


Figure 2. Assumed actual damage extents (stiffness reduction ratios) of the global structure

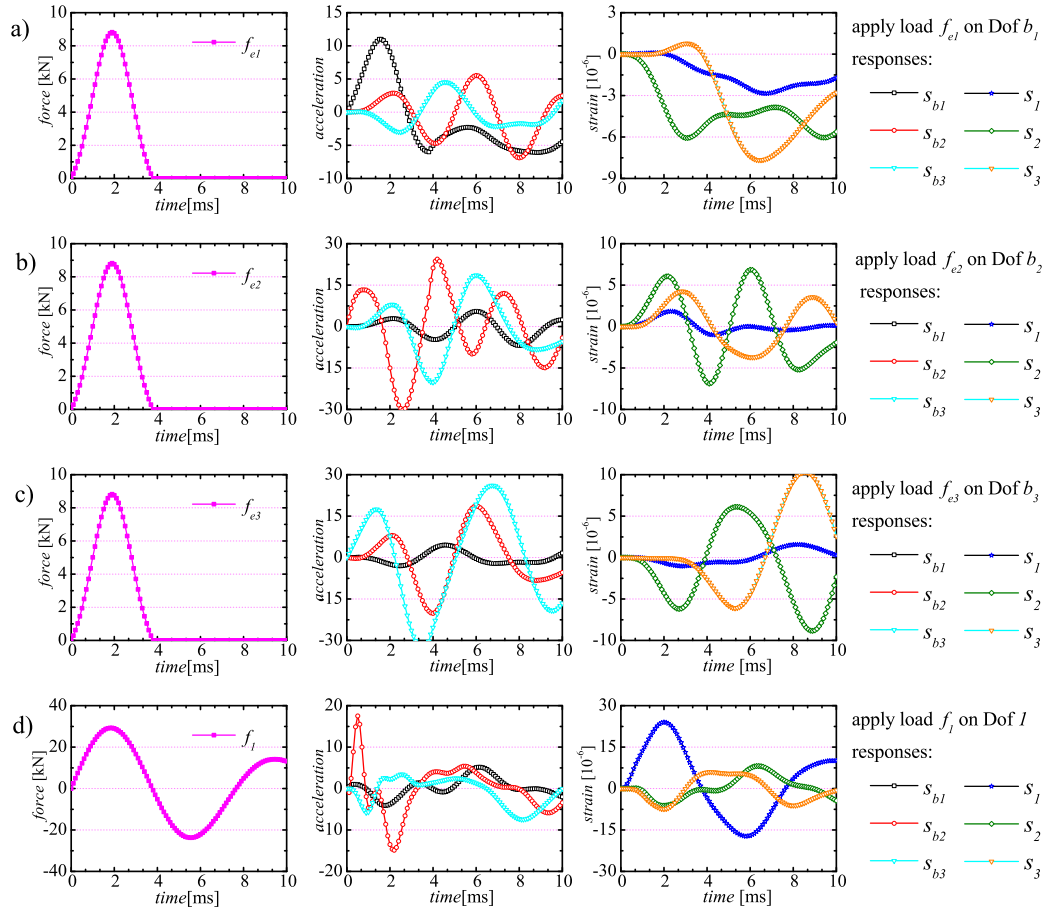


Figure 3. Simulated excitations and the corresponding responses of the entire structure: (abc) Excitations in the boundary DOFs of the substructure, necessary to construct the matrices \mathbf{B} and \mathbf{D} ; (d) Test excitation of the substructure at the location of sensor 1, necessary to obtain \mathbf{a}^M , $\boldsymbol{\varepsilon}^M$ and to compute $\boldsymbol{\varepsilon}$

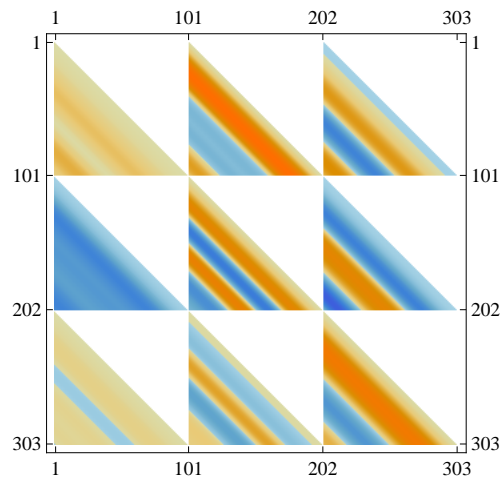


Figure 4. The block Toeplitz structure of the matrix \mathbf{B} used in the numerical example

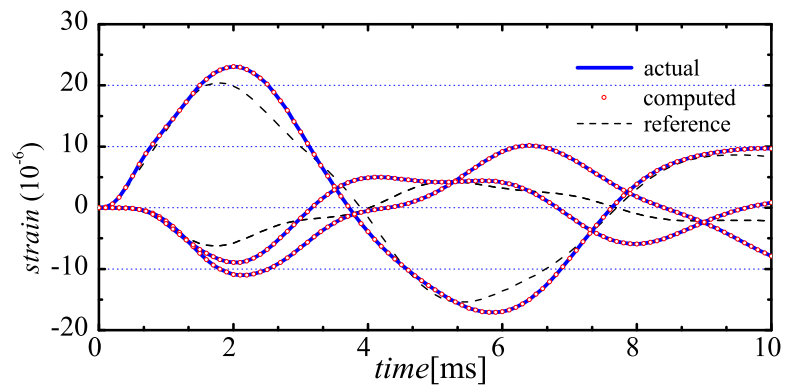


Figure 5. Responses of the damaged isolated substructure to the test excitation at the location of the interior sensors 1, 2 and 3: (solid) computed directly using the assumed damage extents; (dotted) computed by (13); (dashed) reference response of the undamaged isolated substructure

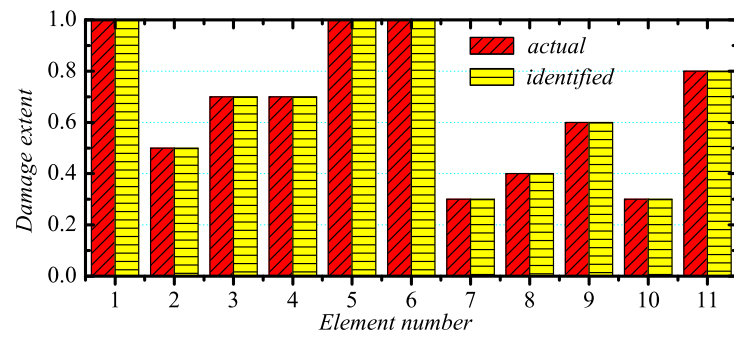


Figure 6. Comparison of the identified and actual damage extents (no simulation of measurement error)

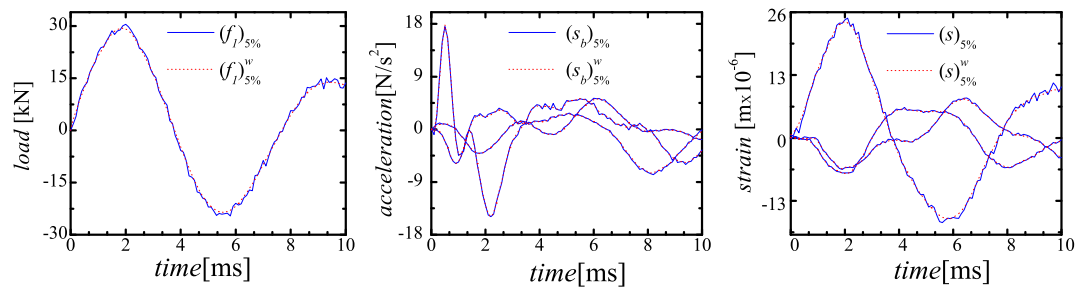


Figure 7. Noise-polluted and denoised excitation and responses corresponding to the noise-free plots of Figure 3(d)

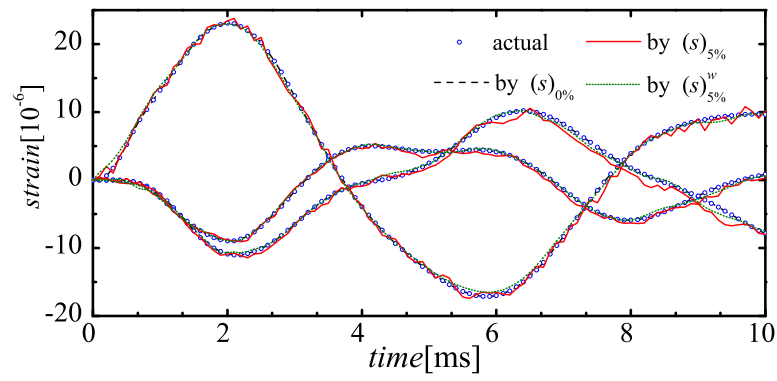


Figure 8. Responses of the damaged isolated substructure to the test excitation, computed using simulated measurements: accurate, noise-polluted and denoised

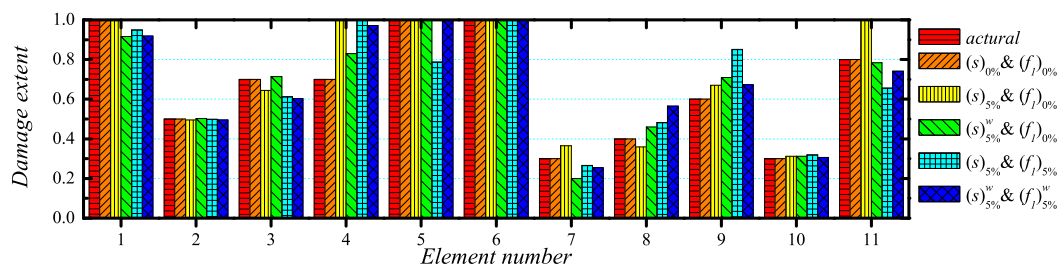


Figure 9. Comparison of the damage extents: actual and identified in the five tested cases of noise pollution